

AD-A047 854

NAVAL OCEAN SYSTEMS CENTER SAN DIEGO CALIF
AEROSOL MEASUREMENTS IN THE MARINE BOUNDARY LAYER AT SAN DIEGO.(U)
NOV 77 D R JENSEN

F70 174

UNCLASSIFIED

NOSC/TR-168

NL

1 OF 1

ADAO47854



END
DATE
FILMED
1 - 78
DDC

12
NOSC

NOSC / TR 168

AD A047854

NOSC / TR 168

Technical Report 168

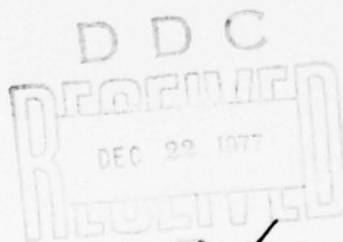
**AEROSOL MEASUREMENTS IN THE
MARINE BOUNDARY LAYER AT
SAN DIEGO**

by
DR Jensen

1 November 1977

Prepared for
Naval Air Systems Command

Research, April 1976 through February 1977



AD No. _____
DDC FILE COPY

Approved for public release; distribution is unlimited

**NAVAL OCEAN SYSTEMS CENTER
SAN DIEGO, CALIFORNIA 92152**



NAVAL OCEAN SYSTEMS CENTER, SAN DIEGO, CA 92152

AN ACTIVITY OF THE NAVAL MATERIAL COMMAND
RR GAVAZZI, CAPT USN **HL BLOOD**

Commander

Technical Director

ADMINISTRATIVE INFORMATION

Work was performed under Naval Environmental Prediction Research Facility Task ZF52551001, Program Element 62759N, Project Number F52551 (NOSC M117) by members of the EM Propagation Division (NOSC Code 532) for the Naval Air Systems Command. This report covers work performed from April 1976 through February 1977 and was approved for publication on 1 November 1977.

METRIC INFORMATION

1 yard = 0.91 metre

1 mile = 1.6 kilometre (approx)

ACKNOWLEDGEMENTS

The author appreciates the discussions with JH Richter, HG Hughes, and VR Noonkester, the assistance of WK Horner, the help of ML Phares with the instrumentation measurements, and the processing of the data by JS Woodward.

Released by
Dr JH Richter, Head
EM Propagation Division

Under authority of
Dr RR Gardner
Associate Department Head
Environmental Sciences
Department

UNCLASSIFIED

SECURITY CLASSIFICATION OF THIS PAGE (When Data Entered)

REPORT DOCUMENTATION PAGE		READ INSTRUCTIONS BEFORE COMPLETING FORM
1. REPORT NUMBER 14 NOSC Technical Report 168 (TR-168)	2. GOVT ACCESSION NO.	3. RECIPIENT'S CATALOG NUMBER 9
4. TITLE (and Subtitle) 6 AEROSOL MEASUREMENTS IN THE MARINE BOUNDARY LAYER AT SAN DIEGO	5. TYPE OF REPORT & PERIOD COVERED Research repl. April 1976-February 1977	
7. AUTHOR(s) 10 DR Jensen	8. CONTRACT OR GRANT NUMBER(s)	
9. PERFORMING ORGANIZATION NAME AND ADDRESS Naval Ocean Systems Center San Diego, CA 92152	10. PROGRAM ELEMENT, PROJECT, TASK AREA & WORK UNIT NUMBERS 16 17 62759N F52551 ZF52551001 (NOSC M117)	
11. CONTROLLING OFFICE NAME AND ADDRESS Naval Air Systems Command Washington, DC 20360	12. REPORT DATE 11 1 November 1977	
14. MONITORING AGENCY NAME & ADDRESS (if different from Controlling Office) 12 23p.	13. NUMBER OF PAGES 22	
15. SECURITY CLASS. (of this report) Unclassified		15a. DECLASSIFICATION/DOWNGRADING SCHEDULE
16. DISTRIBUTION STATEMENT (of this Report) Approved for public release; distribution is unlimited.		
17. DISTRIBUTION STATEMENT (of the abstract entered in Block 20, if different from Report)		
18. SUPPLEMENTARY NOTES		
19. KEY WORDS (Continue on reverse side if necessary and identify by block number) Aerosols, Electro-Optics Extinction Coefficients		
20. ABSTRACT (Continue on reverse side if necessary and identify by block number) The temporal and spatial variability of the aerosol size distribution in the marine boundary layer for different meteorological conditions has been determined using fixed ground based and airborne aerosol size spectrometers. The horizontal and vertical variability of the distributions and corresponding calculated extinction coefficients, and the total liquid water content for both clear air and for a Santa Ana related fog event are discussed. ←		

DD FORM 1 JAN 73 1473

EDITION OF 1 NOV 65 IS OBSOLETE
S/N 0102-LF 014-6601

UNCLASSIFIED

SECURITY CLASSIFICATION OF THIS PAGE (When Data Entered)

393-159

B

OBJECTIVE

To determine the temporal variability of the aerosol size distributions in the marine boundary layer for different meteorological conditions like clear air and fog by using an airborne aerosol size spectrometer. In particular, these measurements will be used to aid in the development of maritime aerosol models that adequately describe the size distribution of aerosol scatters.

RESULTS

1. In general, particle sizes and densities decrease with height. However, the vertical profiles of the cumulative aerosol size distribution in clear air show an enhancement of aerosols below the base of the inversion. Above the inversion, the vertical profiles are well described by a power law.
2. Vertical and horizontal variability of the aerosol size distribution for both clear air and fog showed changes in the calculated extinction coefficients ranging over two to three orders of magnitude.
3. Within the Santa Ana related fog, particle diameters exceeded the maximum observable range of the Knollenberg Probe ($29.4 \mu\text{m}$). In clear air, particle diameters never exceeded $4 \mu\text{m}$.
4. Aerosol size distributions obtained within fog by the aircraft are well described as exponential distributions.
5. The cumulative aerosol size distributions for $D \geq 0.45 \mu\text{m}$ appear to be horizontally homogeneous; however, this does not imply horizontal homogeneity of the individual aerosol size spectra.

RECOMMENDATIONS

1. Relate measured aerosol distributions and calculated extinction coefficients to electro-optics (EO) propagation measurements.
2. Make airborne spectrometer measurements for a comprehensive data base of aerosol size distributions in different meteorological conditions to aid in the development of aerosol models which will adequately describe the horizontal and vertical variability of the aerosol size distributions.
3. Make fixed position, surface based aerosol distribution measurements to determine the temporal variability of the aerosol scatters in clear skies, fog, and haze.
4. Determine the characteristic differences between continental and marine aerosols by making airborne spectrometer measurements over coastal regions.
5. Extend the maximum observable range of the Knollenberg spectrometer ASSP-100 to determine the aerosol size distribution above $29.4 \mu\text{m}$ in fogs and clouds.
6. Investigate the seasonal variations of the aerosol size distributions and related extinction, scattering, and absorption coefficients.
7. Make simultaneous remote and direct sensor observations of meteorological parameters and aerosol size distributions to determine any existing relationships.

CONTENTS

INTRODUCTION . . . page 5

PROCEDURE . . . 5

OBSERVATIONS . . . 10

Clear Skies . . . 10

Santa Ana Fog . . . 14

CONCLUSIONS . . . 21

REFERENCES . . . 21

ILLUSTRATIONS

1. Axially scattering spectrometer probe ASSP-100 . . . page 6
2. Aircraft installation of spectrometer probe . . . 6
3. Aircraft installation of spectrometer electronics . . . 7
4. Geometrical configuration for NOSC aircraft spectrometer operation . . . 10
5. Vertical variability of the cumulative aerosol size distribution in clear air, 19 January 1977 . . . 11
6. Vertical variability of the calculated extinction coefficient and total liquid water content for the aerosol size distribution of figure 5, 19 January 1977 . . . 11
7. Horizontal variability of the cumulative aerosol size distribution in clear air at 300m above mean sea level (MSL), 19 January 1977. . . 12
8. Horizontal variability of the calculated extinction coefficient and total liquid water content for the aerosol size distribution of figure 7, 19 January 1977. . . 12
9. Horizontal variability of the cumulative aerosol size distribution in clear air at 37m above MSL, 19 January 1977 . . . 13
10. Horizontal variability of the calculated extinction coefficient and total liquid water content for the aerosol size distribution of figure 9, 19 January 1977 . . . 13
11. Vertical variability of the cumulative aerosol size distribution within a Santa Ana fog, 15 February 1977. . . 16
12. Vertical variability of the calculated extinction coefficient and total liquid water content for the aerosol size distribution of figure 11, 15 February 1977 . . . 16
13. Aerosol size distributions obtained in clear air (profiles at 277 and 168m) and during a Santa Ana fog (profiles at 95 and 166m), 15 February 1977. . . 17
14. Horizontal variability of the cumulative aerosol size distribution within a Santa Ana fog, 15 February 1977 . . . 18
15. Vertical variability of the calculated extinction coefficient and total liquid water content for the aerosol size distribution of figure 14, 15 February 1977 . . . 19
16. Horizontal variability of aerosol size distributions taken at 0.4km intervals during a Santa Ana fog, 15 February 1977 . . . 20

TABLES

1. Knollenberg aerosol size spectrometer specifications . . . page 8
2. Aerosol size distribution data format . . . 9

ACCESSION for	
NTIS	<input checked="checked" type="checkbox"/>
DDC	<input type="checkbox"/>
UNANNOUNCED	<input type="checkbox"/>
JUSTIFICATION	
BY	
DISTRIBUTION/AVAILABILITY NOTES	
DI	

[Handwritten signature/initials over the bottom section of the form]

INTRODUCTION

Existing and proposed EO systems for surveillance, communication, range finding, tracking, and target designation must contend with the highly variable visible and infrared propagation characteristics of the marine boundary layer (MBL).^{*} Currently, the Navy does not have the capability to evaluate in real time the effects of atmospheric aerosols and inhomogeneities in their concentrations on the performance of Navy EO systems. Techniques are needed to predict the performance of these systems in such meteorological conditions as clear air, fog, and haze.

EO propagation predictions in the marine environment require aerosol models that adequately describe the size distribution of the aerosol scatterers. Data from in-situ measurements of these aerosol size distributions have been described analytically,¹⁻³ and together with Mie scattering theory⁴ have provided a method for estimating an optical range. However, these models were developed from point measurements and do not account for the horizontal and vertical variability of the aerosol size distribution along the propagation path. In propagation assessments, horizontal homogeneity and standard vertical lapse rate of aerosol size distributions are usually assumed. Deviations from such assumptions can significantly alter the effective range of EO systems and consequently degrade the system performance.

In April 1976, two Knollenberg drop-size spectrometers were purchased from Particle Measuring System, Inc (PMS), Boulder, Colorado, by NOSC to make fixed ground based and airborne aerosol size distribution measurements in the MBL to determine the temporal and spatial variability (both horizontally and vertically). It is the purpose of this report to present aircraft observations showing the horizontal and vertical variability of the aerosol size distributions and corresponding calculated extinction coefficients and total liquid water contents for both clear air and Santa Ana related fog events.

PROCEDURE

Measurements of the horizontal and vertical variability of the aerosol size distributions in the MBL have been made using an aircraft mounted Knollenberg ASSP-100 aerosol size spectrometer. A complete description of the axially scattering spectrometer probe, figure 1, has been given by Dytch.⁵ Specifications for the ASSP-100 are shown in table 1.^{**} The aircraft installation of the spectrometer is shown in figure 2. The spectrometer probe is mounted in the free airstream on top of a Piper Navajo aircraft. Figure 3 shows the installation of the electronics and the data acquisition system within the aircraft. The spectrometer

* Considered here to be below about 2 km.

** Since it is not the intent of this report to make an analysis of or to describe the characteristics and operation of the Knollenberg spectrometer, the interested reader is referred to reference 5.

1. Deirmendjian, D, Scattering and Polarization Properties of Water Clouds and Hazes in the Visible and Infrared, Appl Opt, v 3, No 2, p 187-196, 1964
2. Junge, C, Air Chemistry and Radioactivity, Academic Press, p 382, 1963
3. Junge, C, The Size Distribution and Aging of Natural Aerosols as Determined from Electrical and Optical Data on the Atmosphere, J of Meteor, v 12, p 13-25, February 1955
4. Hulst, HC Van de, Light Scattering by Small Particles, John C Wiley & Sons, New York, 1957
5. Dytch, HE, NJ Carrera, Cloud Droplet Spectrometry by Means of Light-Scattering Techniques, Atmospheric Technology, No 8, p 10-16, spring 1976



Figure 1. Axially scattering spectrometer probe ASSP-100.



Figure 2. Aircraft installation of spectrometer probe.

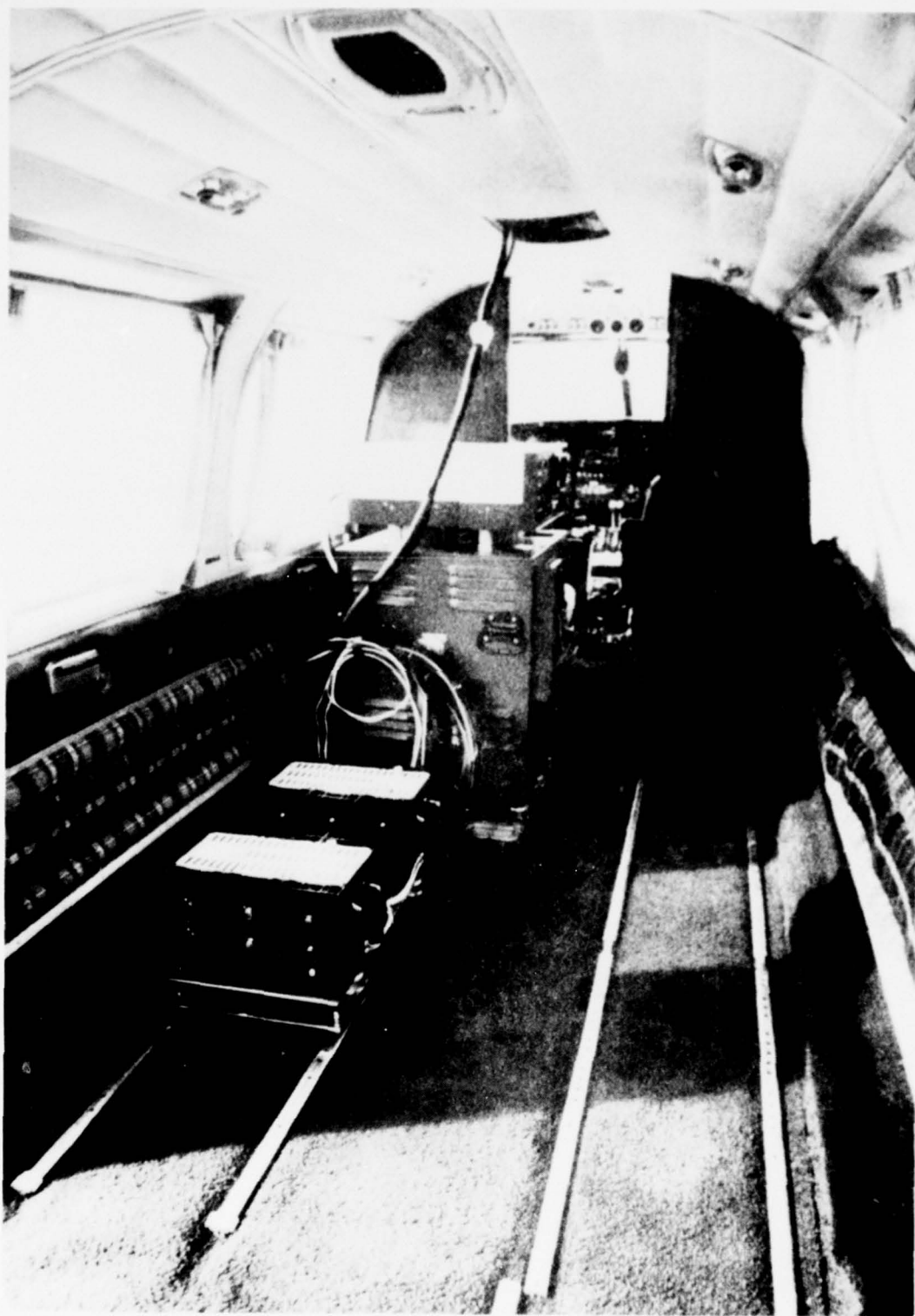


Figure 3. Aircraft installation of spectrometer electronics.

TABLE 1. KNOLLENBERG AEROSOL SIZE SPECTROMETER SPECIFICATIONS.

Size Range: 1) 0.45 - 5.9 μ ; 2) 0.5 - 7.9 μ ; 3) 0.7 - 16 μ ; 4) 1.2 - 29.4 μ
Channels: 15 per range
Resolution: 0.45 μ , 0.5 μ , 0.7 μ , and 1.2 μ for ranges 1, 2, 3, and 4, respectively
Maximum Particle Rate: 100 kHz (125 m/s aircraft) 5 kHz (ground)
Coincidence Errors: Less than 1% with concentration of 10 per cm^3
Output: Analog; digital (18 line parallel BCD and incremental tape recorder)
Laser: He-Ne-TEM01 (632:Å)

data are recorded on a Kennedy 1600/360, incremental, one-half inch, nine-channel magnetic tape recorder. The spectrometer sizes particles from 0.45 μm to 29.4 μm in four range bands with 15 channels per band. The system sequentially steps from range one to range four in 4 seconds and outputs a spectrum of 15 size channels every second (one 15 size channel spectrum for each range band). By combining the data for each range band and eliminating the channel overlap, a 32 channel spectrum from 0.45 to 29.4 μm can be obtained every 4 seconds. Particle density per unit volume per micrometre interval and the cumulative densities greater than or equal to a given diameter can be calculated by using the particle count per unit time, the sampling area, and the aircraft speed. Also, from the known distribution, the total liquid water content contained within the size band of 0.45 to 29.4 μm is obtainable by integrating the absolute drop size distribution for each spectrum. The total scattering, absorption, and extinction coefficients for a given optical wavelength may be calculated by integrating the Mie single-particle cross sections over the appropriate distribution. All data were processed using a Nova 800 computer. The data format is shown in table 2.

The horizontal and vertical profiles of the aerosol size distribution, extinction coefficient, and total liquid water content were obtained in the MBL by flying the aircraft in spirals, slant radials, and constant altitude radials in a wide range of visibilities. The aircraft flew at airspeeds ranging from 60-80 m sec^{-1} and at altitudes ranging from 15 to 600m above MSL. On all spirals and slant radials, the ascent and descent rate was approximately 1 to 2 m sec^{-1} . Figure 4 shows the geometrical configuration for the NOSC aircraft operation. All flights were made in the vicinity of a 286°T radial between San Diego and San Clemente Island.

TABLE 2. AEROSOL SIZE DISTRIBUTION DATA FORMAT.

KSPEC DATA AIRCRAFT

17 FEB 77 14:23:28- 14:25:00 Z

KNOLLENBERG DATA			(VOL= 342.00 CM**3)	WATER CONTENT	
CHL	DIA	COUNTS	DENSITY	GM/CM**3/BW-INT	N (>D) CM**3
1	0.6	7168.7	0.6987039E 2	0.6086499E-11	0.9034792E 2
2	0.9	8351.2	0.8139574E 2	0.2617248E-10	0.6938680E 2
3	1.2	6470.2	0.6306241E 2	0.5021705E-10	0.4496808E 2
4	1.5	4789.4	0.4668033E 2	0.7451183E-10	0.2604936E 2
5	1.7	2643.3	0.2576315E 2	0.7229360E-10	0.1204526E 2
6	2.1	517.0	0.4319131E 1	0.1948250E-10	0.4316317E 1
7	2.4	253.0	0.2113617E 1	0.1529843E-10	0.2804621E 1
8	2.7	200.2	0.1672514E 1	0.1821186E-10	0.2064855E 1
9	3.2	143.0	0.1194653E 1	0.1955060E-10	0.1479474E 1
10	3.5	90.2	0.6593568E 0	0.1480169E-10	0.1061345E 1
11	3.9	45.1	0.3296784E 0	0.1023932E-10	0.7976024E 0
12	4.3	33.0	0.2144249E 0	0.8926217E-11	0.6657310E 0
13	4.7	40.7	0.2644575E 0	0.1483963E-10	0.5692398E 0
14	5.2	35.2	0.2058480E 0	0.1559589E-10	0.4502339E 0
15	5.7	26.4	0.1543860E 0	0.1536732E-10	0.3473099E 0
16	6.3	25.3	0.1345029E 0	0.1760918E-10	0.2701169E 0
17	6.9	18.7	0.9113061E -1	0.1567464E-10	0.1961403E 0
18	7.6	17.6	0.7351714E -1	0.1656594E-10	0.1414619E 0
19	9.4	5.5	0.1461988E -1	0.6256989E-11	0.8999985E -1
20	10.5	11.0	0.2923977E -1	0.1747065E-10	0.7391798E -1
21	11.5	6.6	0.1929824E -1	0.1536730E-10	0.4175429E -1
22	12.5	2.2	0.6432749E -2	0.6578292E-11	0.2245605E -1
23	13.5	5.5	0.1608187E -1	0.2071687E-10	0.1602329E -1
24	14.5	0.0	0.0000000E 0	0.0000000E 0	-0.5857568E -4
25	15.5	0.0	0.0000000E 0	0.0000000E 0	-0.5857568E -4
26	17.2	0.0	0.0000000E 0	0.0000000E 0	-0.5857568E -4
27	19.1	0.0	0.0000000E 0	0.0000000E 0	-0.5857568E -4
28	21.0	0.0	0.0000000E 0	0.0000000E 0	-0.5857568E -4
29	22.9	0.0	0.0000000E 0	0.0000000E 0	-0.5857568E -4
30	24.7	0.0	0.0000000E 0	0.0000000E 0	-0.5857568E -4
31	26.6	0.0	0.0000000E 0	0.0000000E 0	-0.5857568E -4
32	28.4	0.0	0.0000000E 0	0.0000000E 0	-0.5857568E -4

TOTAL WATER CONTENT OF AIR (GRAMS/CM**3)= 0.4978327E -9

COMPUTED EXTINCTION, SCATTERING, AND ABSORPTION COEFFICIENTS (KM**-1)
FOR LAMBDA= 0.5300

N= 1.3315000 -J 0.1620000E -8

BETA E= 0.16789310E 0, BETA S= 0.16789310E 0, BETA A= 0.00000000E 0

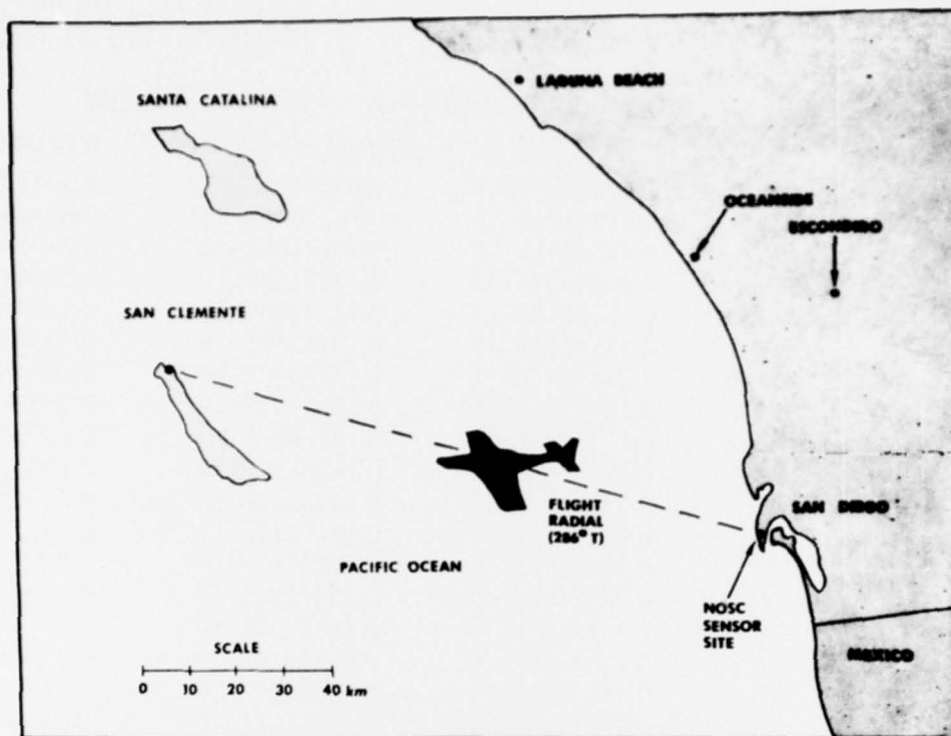


Figure 4. Geometrical configuration for NOSC aircraft spectrometer operation.

OBSERVATIONS

CLEAR SKIES

Airborne spectrometer measurements made in clear air are presented in figures 5-10. Figure 5 shows the vertical variability of the cumulative aerosol size distribution (N) on 19 January 1977 for a visibility ≥ 24 km (measured by the MRI Visiometer Model 1580A). The distribution was measured approximately 1 km off-shore from NOSC by making a spiral ascent from 30 to 600 m. Plotted on the left side of figure 5 is the 2305 GMT standard US Weather Bureau radiosonde taken at Montgomery Field (located approximately 18 km northeast of NOSC and designated by MYF). A temperature inversion exists at 183 m. Below the inversion at 30 m, the cumulative distribution for particles whose diameter (D) is equal to or greater than $0.45 \mu\text{m}$ was $8.7 \text{ particles cm}^{-3}$. Above the inversion, N reached a minimum count of 0.288 cm^{-3} at 400 m and again at 600 m. The overall decrease in the particle density from 30 to 600 m showed a general trend toward smaller drops with height and is well described as a vertical power-law density (N) decrease. From 100 m to the base of the inversion at 183 m, the number density increased indicating aerosol accumulation below the inversion. This accumulation could greatly affect predicted EO propagation characteristics for either vertical or slant radial paths when the analytical aerosol models do not account for such vertical fluctuations. Figure 6 shows the corresponding calculated extinction coefficient

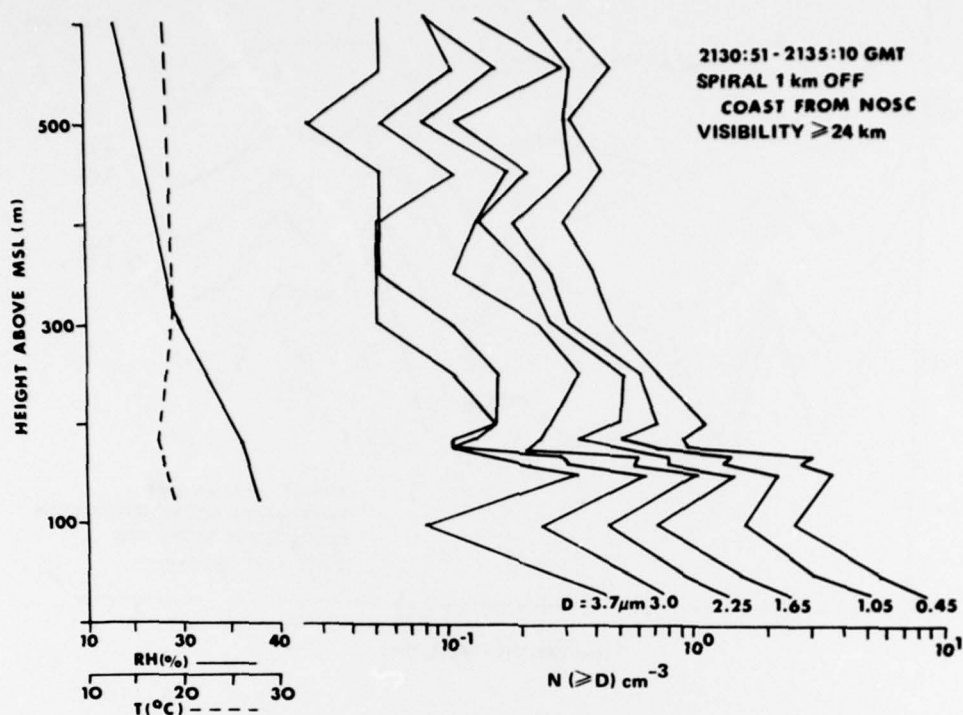


Figure 5. Vertical variability of the cumulative aerosol size distribution in clear air, 19 January 1977.

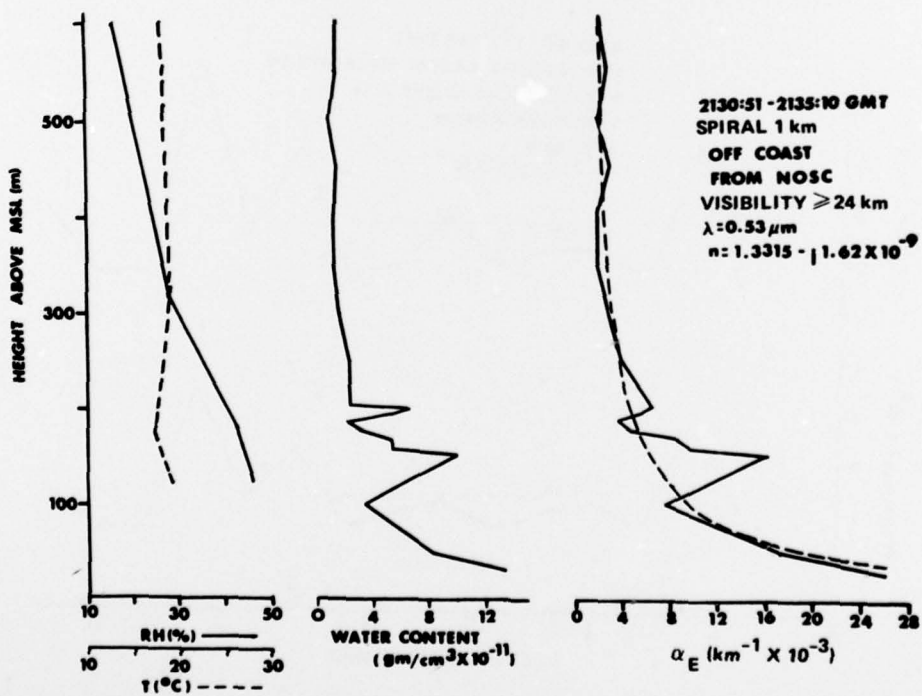


Figure 6. Vertical variability of the calculated extinction coefficient and total liquid water content for the aerosol size distribution of figure 5, 19 January 1977.

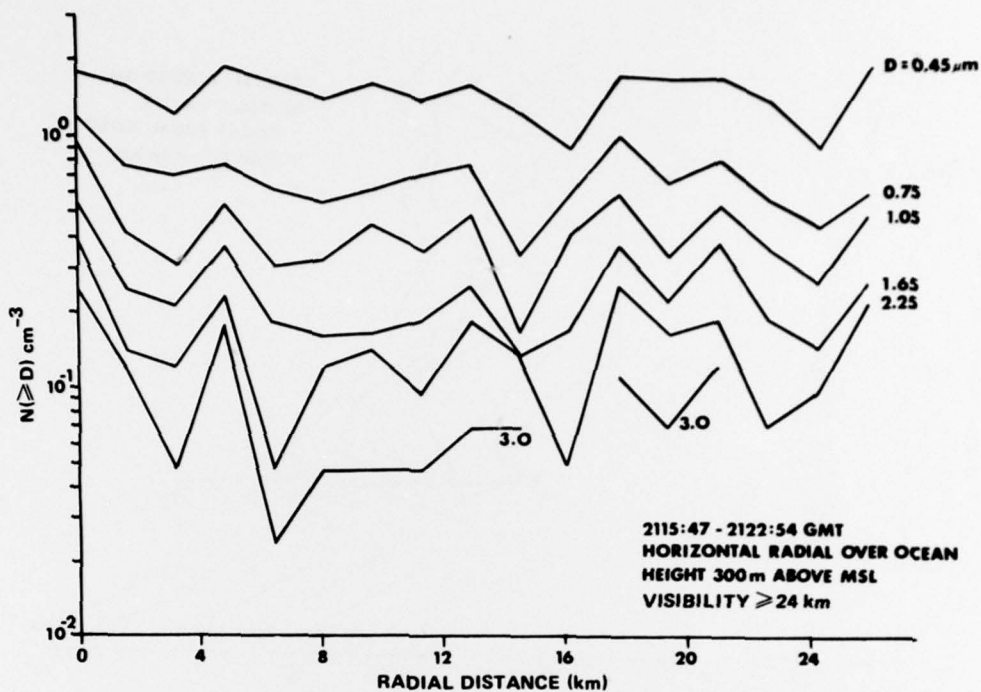


Figure 7. Horizontal variability of the cumulative aerosol size distribution in clear air at 300m above mean sea level (MSL), 19 January 1977.

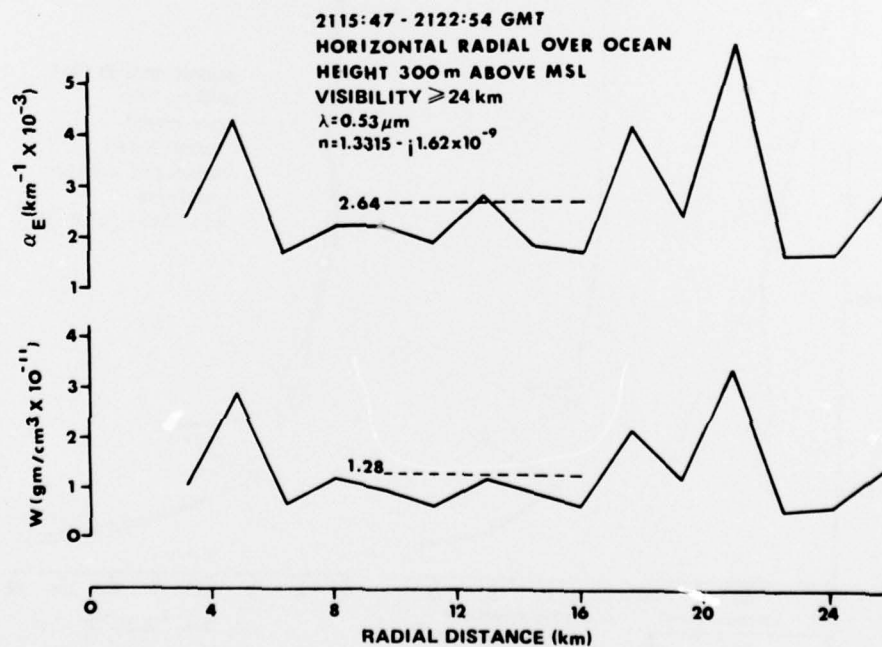


Figure 8. Horizontal variability of the calculated extinction coefficient and total liquid water content for the aerosol size distribution of figure 7, 19 January 1977.

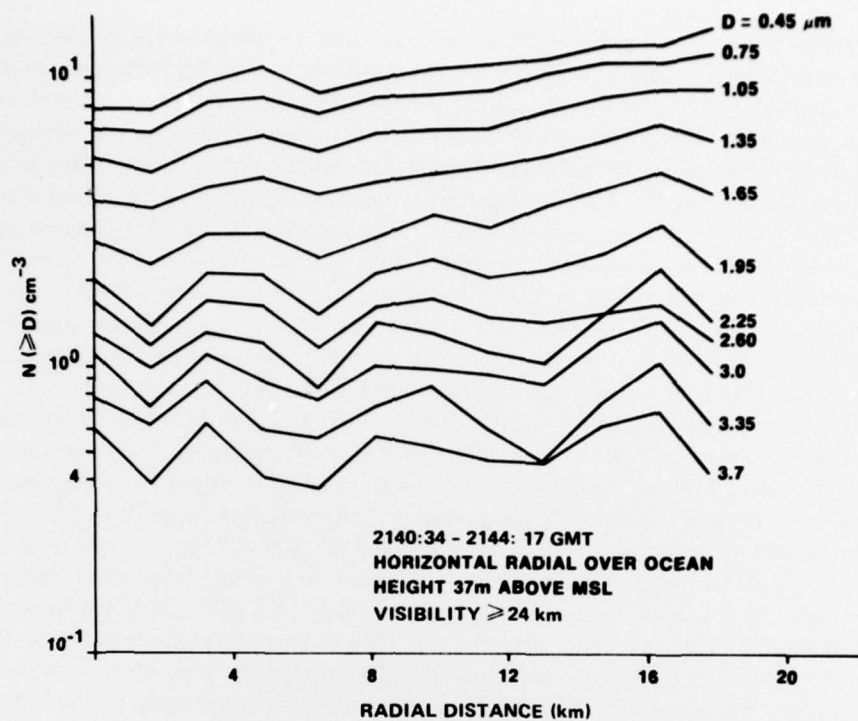


Figure 9. Horizontal variability of the cumulative aerosol size distribution in clear air at 37m above MSL, 19 January 1977.

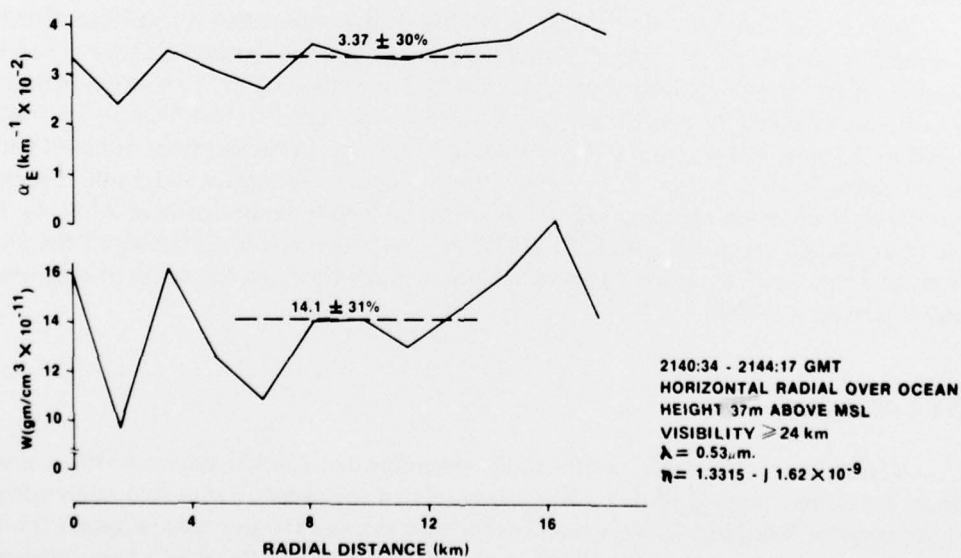


Figure 10. Horizontal variability of the calculated extinction coefficient and total liquid water content for the aerosol size distribution of figure 9, 19 January 1977.

(α_E -solid line) for $\lambda = 0.53 \mu\text{m}$ and the total liquid water content (W) as a function of height for the size distribution shown in figure 5. The 2305GMT local MYF radiosonde data shown in figure 5 is repeated in figure 6 for comparison purposes. The α_E and W curves are similar in appearance since both are obtained by integrating the aerosol size spectra. Below 100m and above 200m, α_E shows a smooth decrease with height. From 100m to the base of the temperature inversion at 183m (region of aerosol accumulation), α_E varied from a minimum of 0.0035km^{-1} to a maximum of 0.016km^{-1} . The dashed line superimposed on α_E is the best fit power law taking into account all measured data points on the α_E curve. The data fit a power law up to 100m and above 200m. However, at 150m, α_E is observed to be 1.66 times larger than would have been predicted by a power law. Therefore, a simple power law model does not always adequately describe the media and EO propagation predictions because there is the possibility that the vertical or slant radial sightings could be inaccurate.

The horizontal variability of the cumulative aerosol size distribution for clear air above an inversion (visibility $>24\text{km}$) over a 26km path is shown in figure 7. Profiles were obtained by flying the aircraft above the inversion (fig 5) at a constant altitude and direction. The cumulative aerosol size distribution for particles with diameters equal to or greater than $0.45 \mu\text{m}$ changed by a factor of two from 0.85 to $1.86 \text{ particles cm}^{-3}$ over the 26km path. For particles with $D \geq 3 \mu\text{m}$, N changed by an order of magnitude from a minimum of 0.023cm^{-3} to a maximum of 0.25cm^{-3} and was not detected from 14.5 to 17.5km nor from 21 km to the end of the 26 km path. For analytical modeling of aerosol size distributions, these results for clear air show that for $D \geq 0.5 \mu\text{m}$ horizontal homogeneity appears to be a good approximation. However, this does not imply horizontal homogeneity of the individual aerosol size spectra since in regions where the number of larger particles decreased, the number of smaller particles increased to maintain a constant N . Since α_E and W are obtained by integrating over the aerosol size distribution, variations in α_E and W would be expected even though the cumulative aerosol size distributions appear to be horizontally homogeneous. Figure 8 shows the horizontal variability of the calculated α_E and W for the constant altitude radial shown in figure 7. Over the 26km path, α_E varied by a factor of two and W changed by a factor of six.

Similar profiles of the horizontal variability of the cumulative aerosol size distribution below the inversion at an altitude of 37m are shown in figure 9. At this altitude N had increased by an order of magnitude over that observed at 300m (fig 5). (The total concentration for $D \geq 0.45\mu\text{m}$ changed by a factor of two, $7.8 \leq N \leq 15.2 \text{ cm}^{-3}$.) However, in contrast, N only changed by a factor of two from 0.73 to 1.44cm^{-3} at 37m. At 300m there were no particles detected above $3 \mu\text{m}$ diameter, however, at 37m the upper size limit was $4.5 \mu\text{m}$. Figure 10 shows the horizontal variability of α_E and W obtained below the inversion at 37m. α_E for $\lambda = 0.53 \mu\text{m}$ varied about the mean of 0.0337km^{-1} by $\pm 30\%$ and W varied about the mean of $14.1 \times 10^{-11} \text{ gm/cm}^3$ by $\pm 30\%$. This variability is much less than the order of magnitude change observed at 300m.

SANTA ANA FOG

Vertical and horizontal profiles of the drop size distribution similar to those made for clear air were also obtained during a Santa Ana related fog event. Santa Ana related fogs form near the coast of Southern California and move into the San Diego region within a few days after the onset of a Santa Ana condition—a condition which occurs when a high pressure region builds over the high elevated plateau along the western states causing dry warm air to move out

over the coastal ocean region. Figure 11 shows the vertical variability of the cumulative aerosol size distribution during the Santa Ana related fog event of 15 February 1977. The profiles were measured on a slant radial (fig 4) while descending from an altitude of 457 to 61m during a time interval of 5 minutes 36 seconds (descent rate of 1.18msec^{-1}). The variability of the particle concentration at the boundary between fog and clear air changed by two orders of magnitude, ie, above the fog at 168m, N for $D \geq 0.45 \mu\text{m}$, varied from 2 to 4 particles cm^{-3} , within the fog (below the billowy tops at 114m) N varied from 267 to 352 particles cm^{-3} . From 114 to 168m the aircraft flew in and out of the billowy tops and the resulting spectra were highly variable; these spectra were not plotted. The 1110 GMT local MYF radiosonde (taken 3 hours before the flight) showed the base of the inversion at 120m, the approximate height where the descending aircraft encountered dense fog. The billows extending up to 168m indicate vertical turbulent mixing near the inversion base. The variability of N above the fog was similar to that for clear air (fig 5). In fog, N increased with height for $0.45 \geq D \geq 11 \mu\text{m}$ but decreased with height for $D > 11 \mu\text{m}$. The corresponding profiles for α_E and W are shown in figure 12. Both α_E and W changed by three orders of magnitude at the transition between clear air and fog. Above the fog (height $\geq 168\text{m}$), α_E decreased according to a power law (dashed curve superimposed on the α_E profile of figure 12); the decrease is similar to that shown in figure 6 for clear skies (no fog below). However, within the fog below the inversion, α_E did not decrease with height but increased slightly from 11.4km^{-1} at 61m to 15.1km^{-1} at 114m.

Characteristic aerosol size distributions obtained in clear air above the Santa Ana related fog at 272 and 168m, and within the fog at 166 and 95m are shown in figure 13. The spectra taken at 272 and 168m in clear air indicate an absence of particles greater than $4 \mu\text{m}$ and are well described as power law distributions with slopes near two. In the fog at 166m (aircraft flying in and out of the billows) and at 95m, a higher density of larger particles was observed; these particles extended out to the maximum size range of the probe ($29.4 \mu\text{m}$) with a peak density occurring at $6.3 \mu\text{m}$. A gap in the density profile at 166m from 7.6 to $17.2 \mu\text{m}$ was created when the aircraft flew out of a fog billow into clear air during the spectrometer sampling period. The decrease in the particle density N for $D \geq 6.3 \mu\text{m}$ in the fog is well approximated by an exponential decay. The large difference between the spectrum at 168 and 166m indicates the presence of a large gradient in aerosols at the fog boundary which creates a three order magnitude change in α_E .

The horizontal variability of the N over a 7.5km path within the Santa Ana related fog is shown in figure 14. N for $D \geq 0.45 \mu\text{m}$ was approximately constant at 300 particles cm^{-3} but for the larger particles ($D \geq 25.6 \mu\text{m}$) it varied from a minimum of 0.25cm^{-3} to a maximum of 1.08cm^{-3} — a change by a factor of four. The corresponding calculated values for α_E ($\lambda = .53 \mu\text{m}$) and W are shown in figure 15. α_E fluctuated about the mean of 1.043km^{-1} by $\pm 37\%$ while W varied about the mean of $6.8 \times 10^{-8} \text{gm cm}^{-3}$ by $\pm 36\%$. These results for the horizontal variability of N within a Santa Ana related fog are similar to those observed in clear air (no fog present) in that N for $D \geq 0.45 \mu\text{m}$ appears to be horizontally homogeneous whereas the corresponding α_E and W are not. Figure 16 shows the horizontal variability of four aerosol size distributions taken at 0.4km intervals along a constant altitude radial within the fog. These spectra are characteristic of a region where N for $D \geq 0.45 \mu\text{m}$ was relatively constant, where N for the larger particles was changing rapidly (fig 14 between 4 and 5.5km), and where α_E and W show large variation (fig 15). The density profiles obtained over the 1.2km path appear to be similar in characteristics. However, for a given diameter, the particle densities changed by as much as a factor of 4 and the peak densities occurred at particle diameters ranging from 1.2 to $3.5 \mu\text{m}$. All four profiles are well described as exponential distributions.

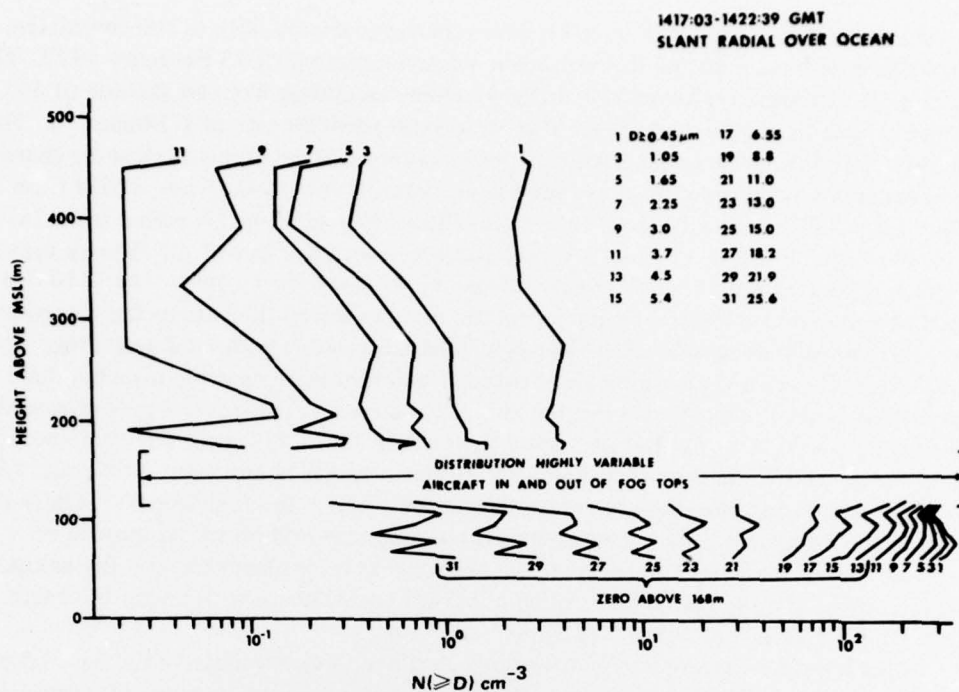


Figure 11. Vertical variability of the cumulative aerosol size distribution within a Santa Ana fog, 15 February 1977.

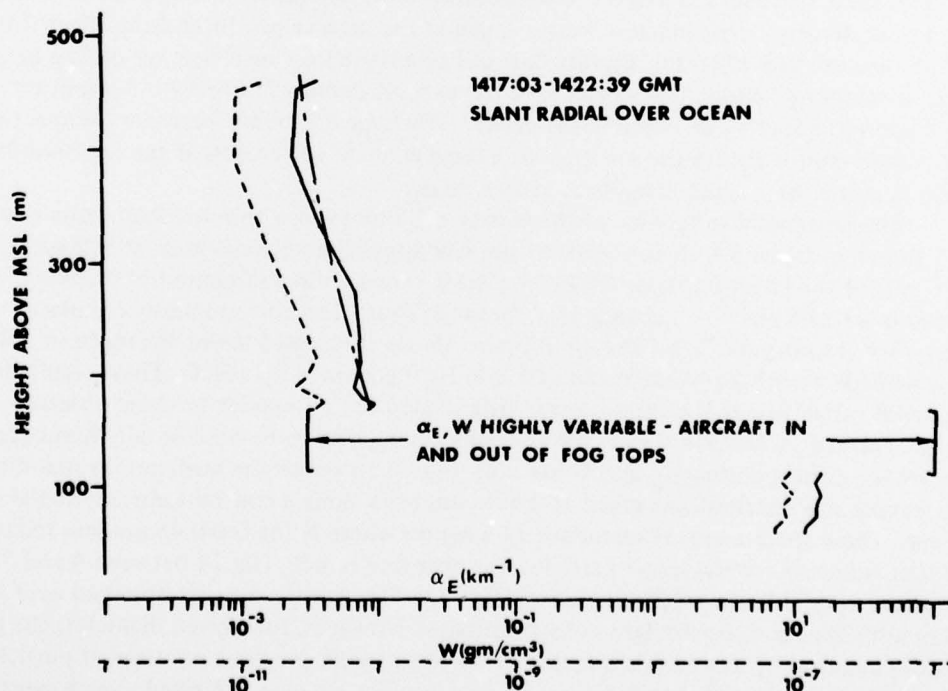


Figure 12. Vertical variability of the calculated extinction coefficient and total liquid water content for the aerosol size distribution of figure 11, 15 February 1977.

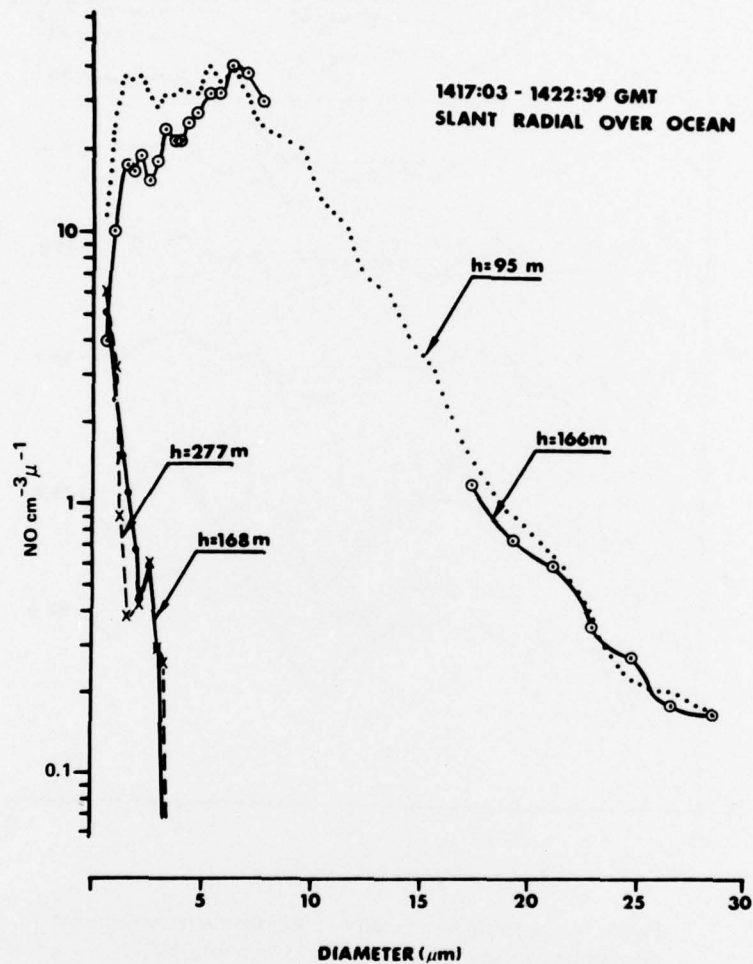


Figure 13. Aerosol size distributions obtained in clear air (profiles at 277 and 168m) and during a Santa Ana fog (profiles at 95 and 166m), 15 February 1977.

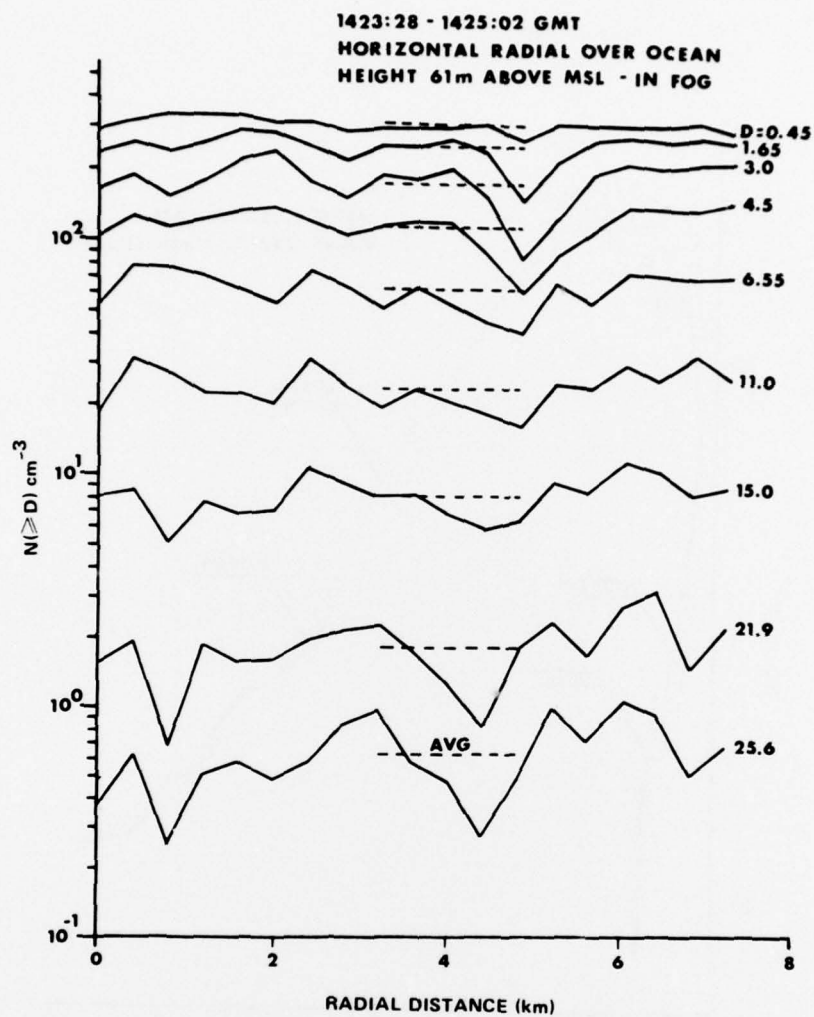


Figure 14. Horizontal variability of the cumulative aerosol size distribution within a Santa Ana fog, 15 February 1977.

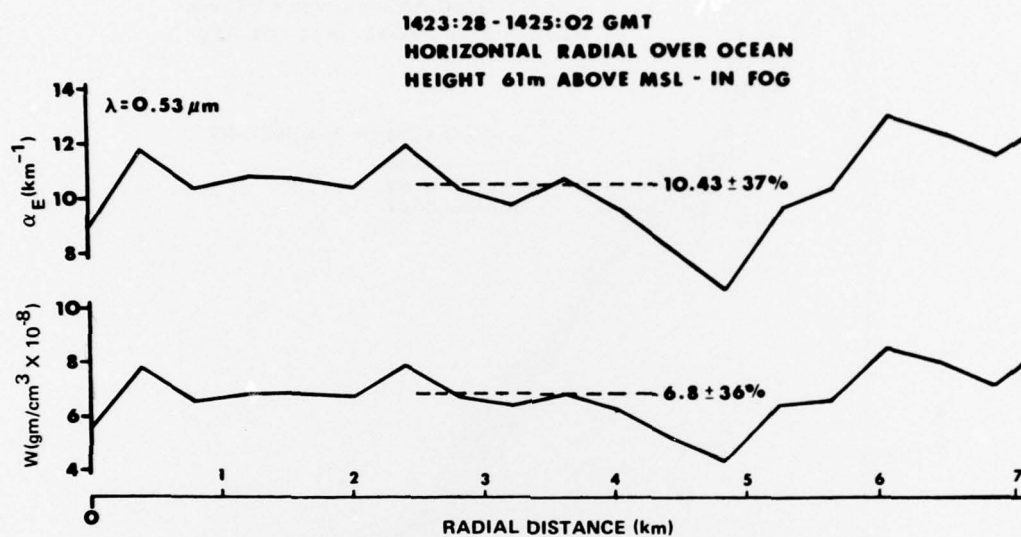


Figure 15. Vertical variability of the calculated extinction coefficient and total liquid water content for the aerosol size distribution of figure 14, 15 February 1977.

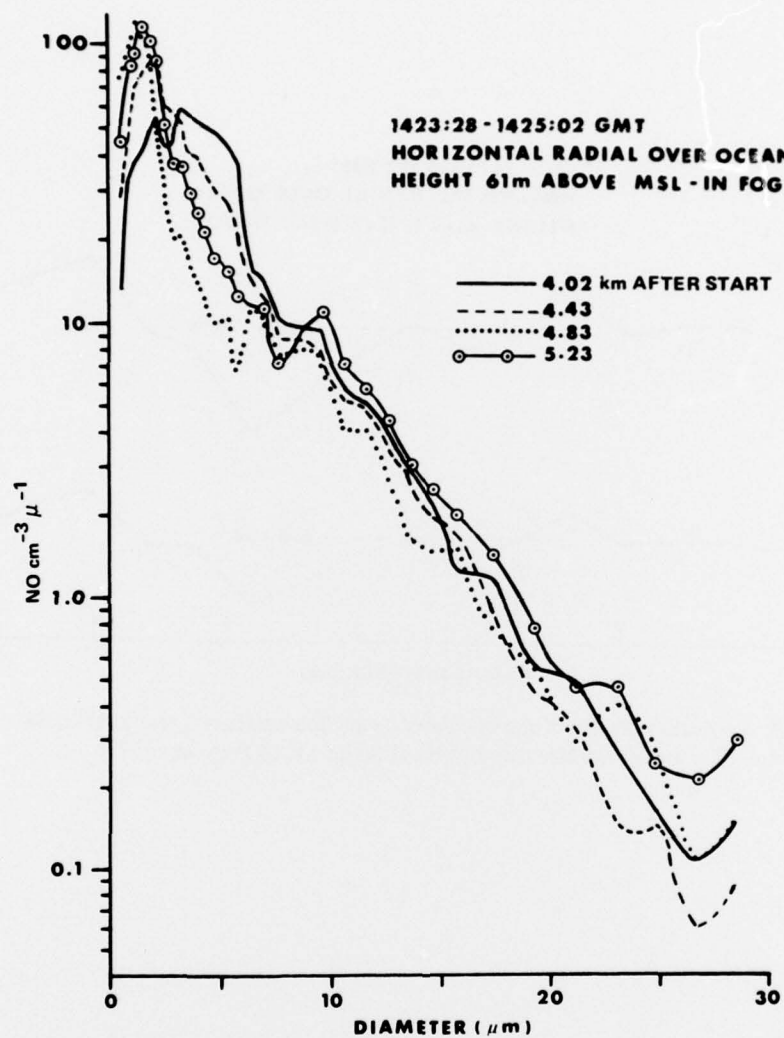


Figure 16. Horizontal variability of aerosol size distributions taken at 0.4km intervals during a Santa Ana fog, 15 February 1977.

CONCLUSIONS

Vertical and horizontal variability of the aerosol size distribution for different meteorological conditions of clear air and fog can seriously affect the prediction of EO system performance. Propagation predictions require aerosol models that adequately describe the size distribution of the aerosol scatterers and must account for the variability of the distributions along the propagation path. Aircraft observations of the vertical and horizontal variability of the aerosol size distribution within clear air and fog show:

1. In general, that particle sizes and densities decrease with height. However, the vertical profiles of the cumulative aerosol size distribution in clear air show an enhancement of aerosols below the base of the inversion. Above the inversion, the vertical profiles are well described by a power law.
2. Vertical and horizontal variability of the aerosol size distribution in the calculated extinction coefficients ranging over two to three orders of magnitude.
3. Within the Santa Ana related fog, the particle diameters exceeded the maximum observable range of the Knollenberg Probe (29.4 μm). In clear air, particle diameters never exceed 4 μm .
4. Aerosol size distributions obtained by the aircraft within the fog are well described as exponential distributions.
5. That the cumulative aerosol size distribution for diameters $D \geq 0.45 \mu\text{m}$ appear to be horizontally homogeneous; however, this does not imply horizontal homogeneity of the individual aerosol size spectra.

REFERENCES

1. Deirmendjian, D, Scattering and Polarization Properties of Water Clouds and Hazes in the Visible and Infrared, Appl Opt, v 3, No 2, p 187-196, 1964
2. Junge, C, Air Chemistry and Radioactivity, Academic Press, p 382, 1963
3. Junge, C, The Size Distribution and Aging of Natural Aerosols as Determined from Electrical and Optical Data on the Atmosphere, J of Meteor, v 12, p 13-25, February 1955
4. Hulst, HC Van de, Light Scattering by Small Particles, John C Wiley & Sons, New York, 1957
5. Dytch, HE, NJ Carrera, Cloud Droplet Spectrometry by Means of Light-Scattering Techniques, Atmospheric Technology, No 8, p 10-16, spring 1976